# Atom ejection from a fast-ion track: A molecular-dynamics study

H. M. Urbassek
*Fachbereich Physik, Universität Kaiserlautern, Erwin-Schrödinger-Strasse, D-67663 Kaiserslautern, Germany*

H. Kafemann
*Institut für Theoretische Physik, Technische Universität, D-38023 Braunschweig, Germany*

R. E. Johnson
*Department of Nuclear Engineering and Engineering Physics, University of Virginia, Charlottesville, Virginia 22901*
(Received 27 August 1992; revised manuscript received 20 July 1993)

As a model for atom ejection from fast-ion tracks, molecular-dynamics simulations of a cylindrical track of energized particles are performed. An idealized situation is studied where every atom in a cylindrical track of radius $R_0$ is energized with energy $E_0$. The emission yield $Y(E_0,R_0)$ shows the existence of two ejection regimes. If the particle energy $E_0$ is below the sublimation energy $U$ of the material, a threshold regime is seen in which $Y$ rises roughly like the third power of $E_0$; for high-energy densities $E_0 \gtrsim U$, the yield rises much more slowly, roughly linearly. In both cases, ejected particles mostly originate from the track, rather than from its surroundings, and from the first or the first few monolayers. The behavior found is interpreted here in terms of emission due to a pressure-driven jet (linear regime) or due to a pressure pulse (threshold regime). These both behave differently from the often-used thermal-spike sputtering model.

## I. INTRODUCTION

When a fast ion penetrates a solid target, it leaves behind a cylindrical *track* of energized atoms.[1] At energies large compared to 25 keV/amu, the ion has only little interaction with individual atomic nuclei of the target, and hence moves on an essentially straight path through the material. However, it excites and ionizes electrons on its path; thus the ion track is essentially a region of high electronic energy density. Electronic excitation can be quickly transferred to atomic motion in this region.[2-7] This atomic motion may lead to long-lasting, visible modifications of the track material,[8] and also to particle ejection from the solid. Such particle emission events may be relevant for all insulating materials; they have been studied in the recent past with particular emphasis on emission of large organic molecules.[2,9-12] In addition, the region excited by lower-energy heavy ions, which can deposit both collisional and electronic energy, may also be well approximated near the surface by a cylindrical energized track, but of larger radius.[13,14]

A number of mechanisms have been proposed to explain particle ejection from cylindrically excited regions. The energy density deposited in the vicinity of the surface may lead to evaporation.[2,13,15,16] On the other hand, the high pressure built up in the track may lead to the ejection of part of the track volume. This idea has been quantified in terms of the "pressure pulse"[17,18] or shock wave[19,20] unloading at the surface and initiating particle emission. In the context of low-energy heavy ion bombardment of volatile targets, the concepts of a "gas flow" of the highly excited material out of the track has been formulated.[14,21]

In the present paper, we wish to study ejection from a cylindrical track region by means of molecular-dynamics computer simulation. We shall use an idealized track model in which the cylinder is homogeneously filled with particles which received a fixed kinetic energy, but random direction of motion. This kinetic energy may have been obtained by a nonradiative electronic relaxation process[16] or directly via momentum transfer.[13] Whether this is truly representative of a particular experimental situation is not essential, as here we use molecular dynamics to study the phase transformation at the surface of an excited cylinder and test proposed analytic models for a well defined example. We use for simplicity Ar as the target material, which is complementary to the diatomics[22] and protein molecules[18] studied previously in the literature. As can be shown by scaling arguments, the ejection yield is only a function of the track radius and the particle energy in the track for such a simple material as Ar; heat conduction, equation of state and other material properties need not be explicitly introduced as further parameters. This is due to the fact that a single length and energy scale completely describe Lennard-Jones interaction; mass only enters to define the time scale of the process. This fact motivated us to perform a study of the ejection yield as a function of the track radius and particle energy in the track.

## II. SYSTEM AND SIMULATION PROCEDURE

We simulate the Ar solid by a cubic block of matter of side length 120 Å, containing 42 592 atoms. All Ar atoms interact via a Lennard-Jones potential

$$V(r)=4\epsilon\left[\left(\frac{\sigma}{r}\right)^{12}-\left(\frac{\sigma}{r}\right)^{6}\right] \quad (1)$$

 

with well depth $\epsilon = 10.32$ meV and length parameter $\sigma = 3.405$ Å. The solid is amorphous. One side of the cube is left free to relax towards the vacuum above it; on the other five sides, heat-conducting boundary conditions are applied[23] to simulate the embedding of our simulation volume in the surrounding material, or on a heat-conducting substrate. The density of Ar in our simulation volume is $n_0 = 0.025$ Å$^{-3}$.

The track is modeled as a cylinder of radius $R_0$ with its axis perpendicular into the solid. At time $t = 0$ all atoms in the cylinder are given the same kinetic energy $E_0$, while the direction of their motion is chosen randomly. In order to prevent atom emission from the back side of the target, the track terminates three atom layers, i.e., 10.2 Å, before the end of the simulation volume, at which our boundary conditions simulate the heat-conducting substrate. In the following, we use scaled quantities for energies and lengths: We scale lengths to the mean interatomic distance $l = n_0^{-1/3} = 3.42$ Å of Ar, and energy to the cohesive (or sublimation) energy $U = 80$ meV.[24] We checked that this energy is reproduced by our simulation.[25]

After time $t = 0$, the time evolution of the atoms in the simulation volume is calculated by a molecular-dynamics code. It uses the Verlet algorithm in velocity form for time integration with a time step between initially 1 fs up to eventually 100 fs for the lowest energy densities. The neighbors of each particle are kept in a neighbor list, which is organized following Ref. 26. The simulation lasts from between 15 ps and 21 ps. Further details of the simulation and the target preparation are published elsewhere.[25]

For each value of $E_0$ and $R_0$, we perform a number of between 25 and 100 simulations in order to obtain statistically significant information. The simulations differ from each other by selecting different cylinder centers in the central region of the surface of our simulation volume.

## III. RESULTS AND DISCUSSION

### A. Ejection yield

In Fig. 1, we display the ejection yield $Y$ (average number of atoms ejected per simulation) as a function of the track radius $R_0$ and the energy per track particle $E_0$. All particles are included, which are at the end of the simulation time (cf. Sec. II) a distance of at least $2.5\sigma$ from the original surface plane. We observe that ejection events can be roughly categorized in two regimes: For large initial particle energies $E_0 \gtrsim U$, the yield rises approximately linearly with $E_0$, $Y \propto E_0^n$ with $n = 0.9 \pm 0.1$; we call this the *linear regime*. This regime has not been identified in any of the earlier simulations. For smaller track particle energies, $E_0 \lesssim U$, the yield rises like a higher power, $Y \propto E_0^n$, with $n = 3.3 \pm 0.2$. We refer to this as the *threshold*[16] or *cubic regime*. The error bars in the above exponents indicate the maximum deviations found in Fig. 1.

As a function of the track radius $R_0$, the yield displayed in Fig. 1(b) exhibits an approximately quadratic behavior, $Y \propto R_0^2$, at the higher excitation densities. At

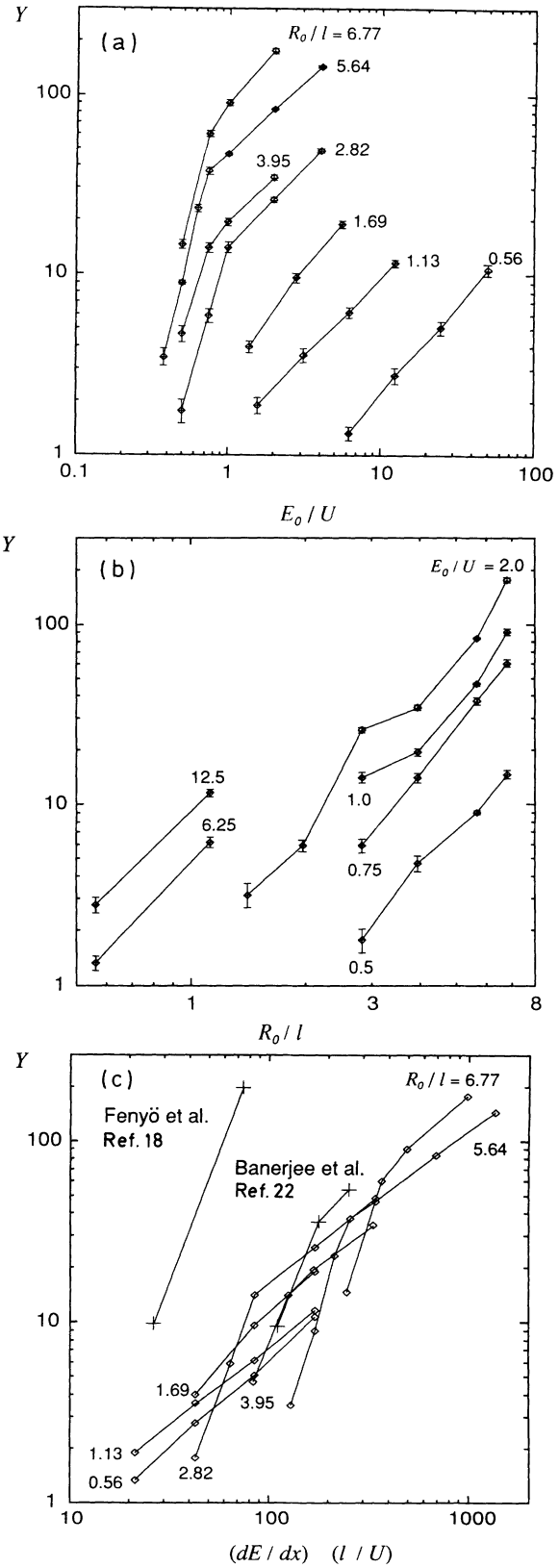


FIG. 1. Ejection yield $Y$ versus (a) energy of track particle $E_0$, versus (b) track radius $R_0$, and versus (c) normalized stopping power. Error bars indicate 1 standard deviation. Symbols (+): Simulation data of Ref. 22, Fig. 3 ($R_0/l \simeq 2.7$), and Ref. 18, Fig. 5(a) ($R_0/l \cong 0.8$) (endnote 46). Lines are guides to the eye.

the critical energy density, $E_0 \cong U$, it shows oscillations, which are definitely out of the statistical error bars of our simulation. At low-energy densities, finally, it is somewhat steeper, approaching a roughly cubic dependence.

For the Lennard-Jones system studied here, besides the particle mass $m$, it is only the Lennard-Jones parameters $\epsilon$ and $\sigma$ which are necessary to describe the material, cf. Eq. (1); for convenience, these latter two may be replaced by the mean interatomic distance $l$ and the cohesive energy $U$. The cylindrical excitation volume is described by its radius $R_0$ and the kinetic energy of an atom, $E_0$. Since $m$, $l$, and $l\sqrt{m/\epsilon}$ provide the mass, length, and time scale of the system, our model system is completely characterized by the dimensionless parameters $R_0/l$ and $E_0/U$. In particular, the yield can depend only on these dimensionless parameters. Separating off the functional dependencies found in our simulations for high-energy densities, we write

$$Y=\frac{l}{U}\frac{dE}{dx}f\left[\frac{R_0}{l},\frac{E_0}{U}\right], \tag{2}$$

where, as is customary,[13,16] the function $f$ describes the threshold behavior. In Eq. (2), we introduced the *effective* stopping power $dE/dx$ of the ion, i.e., the amount of energy per unit depth going into atomic motion. In our model, it has to be set equal to

$$\frac{dE}{dx}=n_0E_0\pi R_0^2 . \tag{3}$$

Thus, our simulations show that $f$ is a slowly varying function of its arguments for $E_0 \gtrsim U$, both for small and large $R_0/l$. For small $E_0/U$ and large $R_0/l$, on the other hand, the calculations show that

$$f\left[\frac{R_0}{l},\frac{E_0}{U}\right]\propto\frac{R_0}{l}\left[\frac{E_0}{U}\right]^2,\quad \frac{E_0}{U}\lesssim 1,\quad \frac{R_0}{l}\gg 1 . \tag{4}$$

The functional dependence of $f$ for $E_0/U \lesssim 1$ *and* small $R_0$ is inaccessible to our simulations, as then the yield becomes vanishingly small.

Figure 1(c) demonstrates the above scaling. It is evident that for $E_0 \gtrsim U$, Eq. (2) describes the yield sufficiently well with a constant $f$ whose value is around 0.05–0.2. Since

$$\frac{dE}{dx}\frac{l}{U}=\frac{E_0}{U}\pi R_0^2 n_0 l \tag{5}$$

is identical to the number of atoms in the first monolayer within the excited track for $E_0 \cong U$, at this critical energy density only the equivalent of around 20% of the first monolayer are emitted.

For a high-energy-density event, we checked whether sample thickness affects our results. To this end, we performed a simulation for $R_0=5.64l$, $E_0=2U$, but where the cylinder track only has a length of half the simulation size, i.e., 60 Å. We found that the average yield only changed by 2%, i.e., within the statistical error.

### B. Specific cases: Ejected particle properties

In order to get more insight into the nature of the ejection mechanism, we studied in more detail two specific cases. For a track radius $R_0=5.64l$, we investigate the case of track particle energy $E_0=0.5U$ (cubic regime) and $E_0=2U$ (linear regime). The track radius has been chosen such that the number of track atoms in the surface layer amounts to $n_0\pi R_0^2 l=100$. In the following we present averages over 25 simulation events for each case. The ejection yield is 9 and 83 in the low- and high-energy-density case, respectively.

In Fig. 2, we show the ejection yields for these two cases as a function of the time $t$ when the atom left the surface plane, of the radial distance $r$ from the cylinder axis and the depth $z$, which describe the original position of an emitted atom, and of the energy $E$ and the angle $\vartheta$, which its trajectory makes with the surface normal, measured at a large distance from the surface. All distributions have been normalized to unit area,

$$\int dt\, Y(t)=\int dE\, Y(E)=\int dr\, rY(r)$$
$$=\int d\cos\vartheta\, Y(\vartheta)=\int dz\, Y(z)=1 . \tag{6}$$

Most of the ejection occurs quite promptly after track excitation, the majority of particles being ejected in the first 1–2 ps. However, a long tail is visible. Although the simulations are run to 15–21 ps we terminate the plot at 9 ps as the remaining contribution is small. It appears that part of the delayed emission is due to late sublimation from hot areas, or particle emission from deeper parts of the crater formed (cf. Fig. 4). It may be speculated that after the time scale of our simulation, very late sublimation might occur, which is stimulated by the relaxation of the highly compressed regions surrounding the ion track (cf. below).

The spatial distribution of emitted atoms shows a clear signature for both bombardment conditions: The overwhelming majority of the ejected particles stem from the cylinder track cross section of area $\pi R_0^2$. While for $E_0=0.5U$, most ejected particles stem from the first monolayer, at higher excitation energies a considerable fraction of ejected atoms originate from the second and third monolayer, and even from below that.

The energy distribution of particles ejected in the high-energy-density case is interesting in that a considerable number of particles show up with energy above the initial energy. This is the signature of interatomic collisions between ejected particles which accelerate one of the collision partners at the cost of the other. As a compensation for these swift particles, the majority of ejected particles have quite low energies, with a maximum at around $1\epsilon$, the Lennard-Jones well depth. In the low-energy-density case, no particles with an energy above that imparted initially to the track atoms are observed; this is plausible. Note also here the slight maximum at $1\epsilon$.

The angular distributions of both events are similar. They deviate strongly from a cosine distribution in that most particles are emitted close to the surface normal. In fact, a best fit to the high-energy-density data of the form

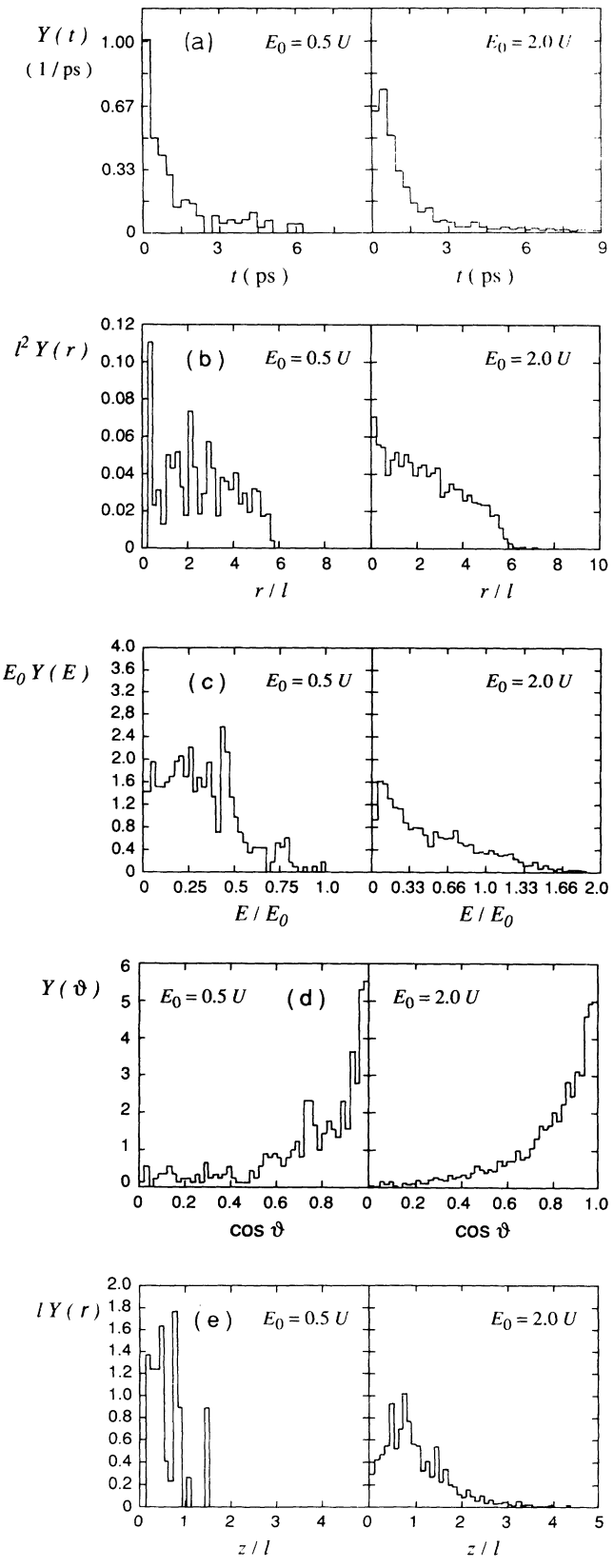


FIG. 2. Ejected particle properties for a low-energy-density case (left hand) and a high-energy-density case (right). (a) Time distribution, $Y(t)$. (b) Spatial distribution, $Y(r)$. (c) Energy distribution, $Y(E)$. (d) Angular distribution, $Y(\vartheta)$. (e) Distribution in depth of origin, $Y(z)$.

$Y(\vartheta) \propto \cos^n \vartheta$ gives a value of $n \cong 2$; we note, however, that the data do not support such a polynomial fit too well. The strongly forward-directed nature of the ejection flow cannot be explained by the formation of an ejection jet proper, since too few atoms are ejected in the low-energy case. Furthermore, when calculating a Mach number $M$ from the energy distributions of Fig. 2(c), a value of $M = 1.6$ results for the high-energy-density case, which means that the flow is only slightly supersonic. It rather appears that the directed emission is due to the strong directed force inducing ejection, viz. the outward pressure gradient (see below), which enforces a preferential direction on the ejection process.

### C. Evolution of solid material for high-energy density case

In Fig. 3, we show the time evolution of several macroscopic variables describing the state of the solid material in and around the track. Only the evolution for the high-energy-density case is shown; below we comment on the evolution of the analogous quantities for the low-energy-density case. We display the simulation results for a typical event. Only the radial dependence is shown, with the origin $r=0$ at the position of the track center, integrating over the depth dependence. Only the particles below the original target surface, rather than the ejected atoms, are included in the quantities shown.

The figure shows the radial distribution of the temperature $T(r,t)$, the pressure $p(r,t)$, the radial component of the velocity $u_r(r,t)$, the density $n(r,t)$, and the potential energy per particle $E_{\rm pot}(r,t)$ at times up to 2.6 ps, when the majority of ejection has taken place. We display scaled variables; the reference quantities are formed from the Lennard-Jones parameters $\epsilon$ and $\sigma$, and the Ar mass $m$. While $n_0$ has been introduced above as the initial density, it is $T_0 = \epsilon/k = 119.8$ K with Boltzmann's constant $k$, $p_0 = \epsilon/\sigma^3 = 0.26$ meV/Å$^3$, and $u_0 = 10.33\sqrt{\epsilon/m} = 16$ Å/ps is the (longitudinal) speed of sound along a cube axis in an fcc Ar crystal.[27–29] For orientation we note that the bulk modulus of Ar is $75 p_0$.[30]

The mean flow velocity $\mathbf{u}$ in a cylinder ring is defined as the average $\langle \mathbf{v} \rangle$ of the velocities of all particles in that ring. The temperature $(3/2)kT = \langle (m/2)(\mathbf{v}-\mathbf{u})^2 \rangle$ measures the kinetic energy per particle available for random motion around the flow velocity; the total kinetic energy per particle then is $(3/2)kT + (m/2)\mathbf{u}^2$. The pressure contains contributions from kinetic- and potential-energy density; we calculate it following common recipes based on the virial theorem.[31]

Let us first discuss the temperature evolution. It is seen that temperature decreases steadily in the cylinder track and is transported outwards. A rough calculation based on the temperature spread plotted, is consistent with a thermal diffusivity of Ar of 140 Å$^2$/ps.[32,27] However, the region outside the cylinder track never achieved a substantial temperature. We note that the melting temperature of Ar is around $T_m/T_0 = 0.7$, while the critical point of the gas-liquid phase transition is at $T_c/T_0 = 1.26$.[32,33] Thus, the regions outside the track predominantly remain in the condensed phase. The track

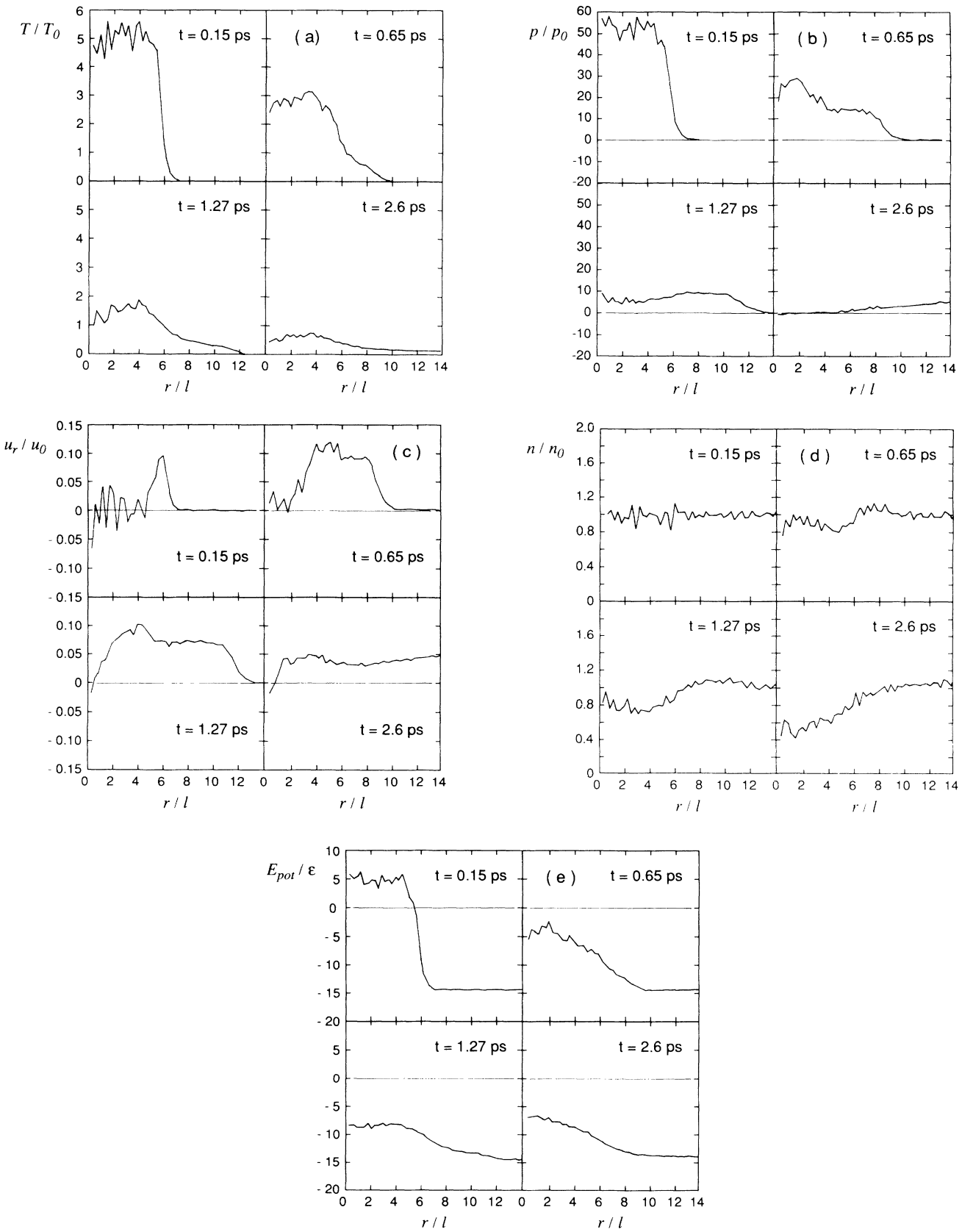


FIG. 3. Time evolution of target material for high-energy-density event. (a) Temperature $T(r,t)$, normalized to the temperature scale $T_0=\epsilon/k$. (b) Pressure $p(r,t)$, normalized to the pressure scale $p_0=\epsilon/\sigma^3$. (c) Radial velocity $u(r,t)$, normalized to the speed of sound $u_0$. (d) Density $n(r,t)$, normalized to the initial density $n_0$. (e) Potential energy per particle $E_{\rm pot}(r,t)$, normalized to the Lennard-Jones energy $\epsilon$.

cylinder itself has a temperature above the critical point in the first 1.3 ps. It is obvious, however, that the concept of a "temperature" need not apply at these early times, since the process started with a non-Maxwellian initial distribution. The high temperatures mean in any case that the binding forces have become small (i.e., the potential energy significantly increased) and the material becomes fluid, cf. also the discussion of the potential-energy distribution below.

As a consequence of the high-energy density in the track region, a high pressure builds up. The figure shows how a pressure pulse expands radially from the track. For this high-energy density, it retains a relatively sharp front, and represents therefore a solid-state shock wave.[25,34,35] It travels with a speed of 20 Å/ps, which is supersonic since the velocity of sound in solid Ar is around 16 Å/ps. At large times, a slight tensile stress develops in the track core, and at $t > 3$ ps in the entire simulation volume (not shown here); it initiates target relaxation towards the crater formed [cf. Fig. 4(c) and discussion below].

Material moves outward from the track as a consequence of this shock wave. While initially a nonvanishing radial velocity develops at the *gradient* of the pressure, the acceleration integrates up with time, and the entire simulation volume expands. Note that the average speed of the atoms is far below the speed of sound $u_0$. This is typical of solid-state shock waves, whose front is supersonic, while atom motion is slow.[34]

The density shows the evacuation of the cylinder track with time. This phenomenon proceeds beyond the times shown, until a huge crater has formed, cf. Fig. 4(c) below. Note the slight (10%) overdensities at $t=0.65$ ps and $t=1.27$ ps, which correlate with the shock wave expansion.

The depth-averaged potential energy per particle $E_{\rm pot}$ is *positive* in the track at the earliest time monitored. This shows that particles acquired such a high energy that they mainly feel repulsive forces between them. While forces become attractive soon again, we note that the potential energy per particle remains substantially less (in absolute magnitude) than the solid equilibrium value of $-14\epsilon$ indicates. The reason hereto lies in the thinning of the track region [cf. Fig. 3(d)] such that particles have less neighbors (or larger interparticle distances) than in the equilibrium solid.

Equipartition of energy requires

$$\frac{3}{2}kT+\frac{m}{2}\mathbf{u}^2\cong\frac{1}{2}(E_{\rm pot}-E^0_{\rm pot})\ , \tag{7}$$

where $E^0_{\rm pot}$ is the potential energy per particle in a system which is at equilibrium at the actual local density and at zero temperature. The factor $\frac{1}{2}$ stems from the fact that when adding all potential-energy contributions in the volume, bonds are counted twice. As discussed above, at late times, $|E^0_{\rm pot}|$ becomes smaller than $14\epsilon$ because of track thinning; hence equipartition is hard to discuss at later times. At the earliest time shown, however, we may neglect the contribution of mass flow, $m\mathbf{u}^2/2$. The kinetic energy thus amounts to around $7.5\epsilon$, while half

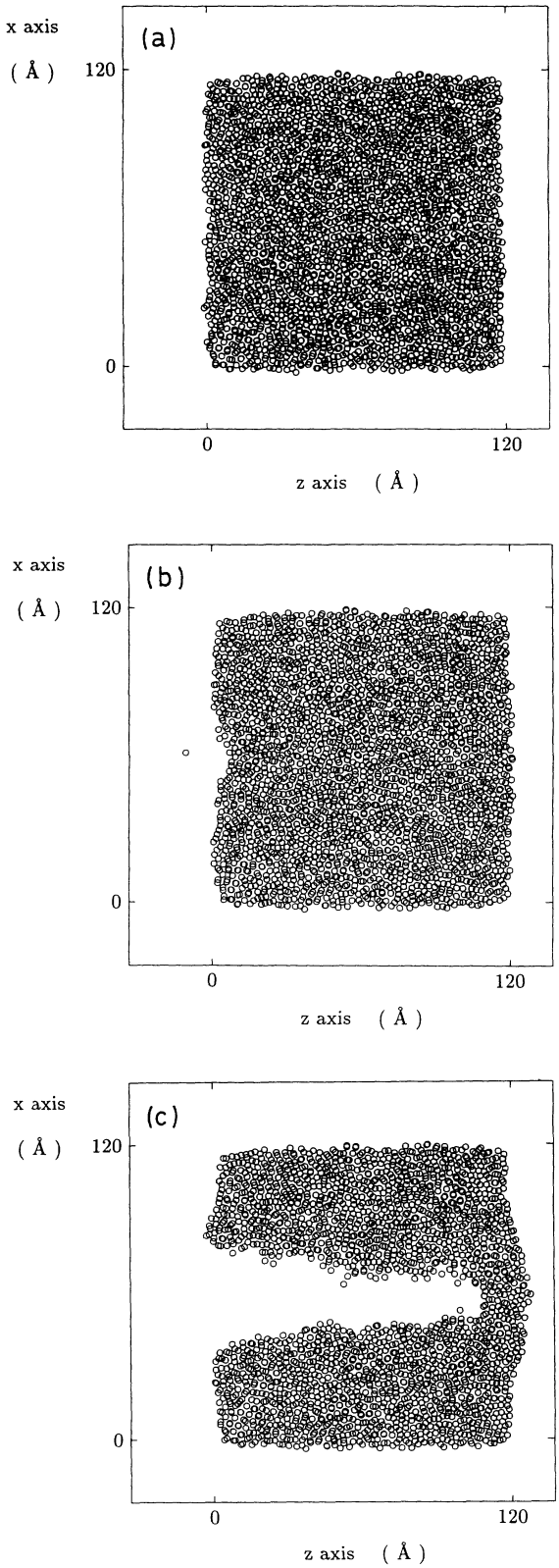


FIG. 4. Original solid before track formation (a), and craters formed in a low-energy-density event (b) and in a high-energy-density event (c). A cross section through the Ar solid is shown, with the initial surface at $z=0$ Å. The cylinder axis of the track is at $x=60.3$ Å and $y=51.6$ Å. Every circle represents an Ar atom in a layer extending 3.5 Å on both sides of the plotted plane, at a time of 5 ps after track excitation (b,c).

the potential-energy increase is around $9.5\epsilon$. We attribute this deviation from equipartition to the oscillations between kinetic and potential energy,[22] which are present in our system at early times, and to the spatial fluctuations in the atomic number density of our amorphous specimen. The sum of kinetic and potential energy is $17\epsilon$, which coincides satisfactorily with the excitation energy of $16\epsilon$.

The corresponding figures for the low-energy-density case (not shown here) display qualitatively the same features, but in a less pronounced way. Thus, at a time of $t=0.22$ ps, the temperature is only close to $T=T_0$, i.e., the track material is always condensed, and the pressure amounts to $p/p_0=18$. Nevertheless, also in this case, a weak shock wave forms, the velocity of which is 16 Å/ps, just around the speed of sound. The material surrounding the track expands, albeit at smaller velocities ($u_r \lesssim 0.07 u_0$) and the density in the track region sinks.

Figure 4 shows an example of the "craters" formed in the low-energy density and in the high-energy density event. Note that this is not the average over 25 events, but a single simulation result. We observe that in the low-density event, the ejected atoms only leave a slight impression on the target surface. This picture is quite consistent with the notion that the ejected atoms (10 in this case) almost exclusively originate from the outermost surface layers in this case of low-energy density, cf. Fig. 2(e). In the high-energy-density event, on the other hand, a large crater is formed which penetrates far into the material. Seventy-six atoms were ejected in this case, and it is obvious that these form only a small fraction of the atoms emptied from the crater. The vast majority of the atoms which initially filled the crater volume have been driven radially into the surroundings. Note that our boundary conditions prevent the crater from going straight through the entire simulation volume: The three last atomic layers were not energized and the heat-conducting boundary conditions strongly "cool" the material there. However, we note that when performing the same simulation with only half as deep a track, the yield is virtually unchanged (cf. Sec. III A). This gives further evidence to the claim that most of the atoms which initially filled the cylinder track have been driven out radially.

In Fig. 5, we present data which allow us to discuss the importance of energy loss from the excited track via ejected particles. For a thick cylinder, $R_0=5.64l$, the average kinetic energy of an ejected particle $E_{\text{eject}}$ is plotted versus the excitation energy $E_0$. In a "free-emission" model, every ejected particle leaves the surface with an energy of $E_{\text{eject}}=E_0-U$. Our data deviate from this law in two respects. First, there is emission for $E_0<U$, i.e., in the threshold regime. Second, the energy of the ejecta does not approach $E_0$ for large $E_0/U$, but appears to saturate at around $(0.4-0.5)E_0$ for $U<E_0<4U$, where our data were taken. This is consistent with the kinetic energy distribution of ejected particles shown in Fig. 2(c), which showed how much particles had slowed down during the expansion process. In the threshold regime, an even more substantial fraction of the excitation energy is lost to the surroundings before and during ejection.

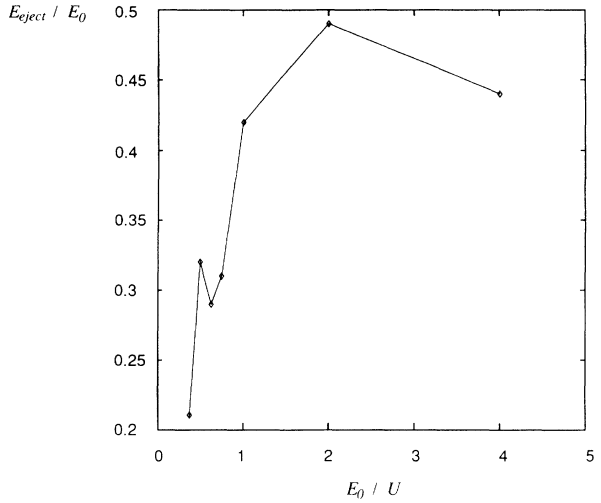


FIG. 5. Average energy $E_{\text{eject}}$ taken away by an ejected particle versus excitation energy $E_0$. Data for a track size $R_0=5.64l$. Lines are guides to the eye.

### D. Comparison with other simulation data

Particle ejection from an energized cylindrical track has been treated by molecular-dynamics simulation previously.[18,22] These simulations differ from the one presented here primarily in that molecules having "structure" and/or possessing internal degrees of freedom were used: Thus Ref. 18 models large organic molecules as spheres which are rapidly expanded in the track, while Ref. 22 treats a target consisting of (pseudo-) $O_2$ molecules which are vibrationally excited in the track region. We extracted the relevant yield data from these latter publications; in the case of $O_2$ molecules we took into account the fact that about 50% of the energy imparted initially to the molecules remains in internal, i.e., vibrational energy, after ejection is completed.

Figure 1(c) shows good agreement between the data of Banerjee *et al.*[22] and our simulation. Also in their data, at low $dE/dx$ the ejecta come predominantly from the excited region. They noted a slower dependence on $dE/dx$ at their "highest" $dE/dx$, which they attributed to their very small sample size. Consequently, they identified the overall dependence as roughly cubic. The fact that their result is slightly shifted to higher $dE/dx$ for a comparable radius can be attributed to the fact that the conversion of internal to center-of-mass energy occurs over a few picoseconds. This is equivalent to a slow, rather than instantaneous, excitation. This was shown in Ref. 36 to shift the yield in the manner seen.

Fenyö *et al.*[18] model the ejection of large organic molecules from an excited track. These authors report ejection yields which rise from $Y\cong 10$ up to 300 if the energy density $l/U\cdot dE/dx$ increases from 15 to 60. Since these data have been obtained for $R_0/l\cong 1$ and $E_0/U\cong 1$, according to Eq. (7) these molecules must have been emitted from deep inside the material. Note that since the molecules are also very large, the volume of material ejected is much larger than that calculated for the material described here. This shows that ejection works quite

differently in this organic-molecule simulation. We attribute this to the fact that the interaction between these large molecules was modeled to have rather a large hard core; only the interaction outside the hard core follows a Lennard-Jones law. As a consequence, the considerable flow of particles *radially* out of the track cylinder, which we observe for Ar, does not occur for these large molecules. That is, this material has a very low compressibility at high excitation densities. Thus, the excited molecules have only one channel to relax the high pressure built up, viz. by ejection into the vacuum. This is the reason that the simulation results of Fenyö *et al.* are one order of magnitude higher than ours and follow the cubic scaling. This shows a decisive influence of the interaction potential on the simulations, and must be taken as a warning.

### E. Comparison with models

A number of models have been formulated to understand the ejection of particles from energetic tracks.[16]

(1) *Spikes*: The high-energy density may lead to evaporation or sublimation from the surface.[13,37–40] Heat conduction to the surroundings and evaporation cooling[41] terminate the process.

(2) *Gas flow*: If the energy density is so high that the material in (part of) the collision cascade volume is above the critical point of the liquid-gas phase transition, matter flows out freely into the vacuum above the surface.[14,21,42]

(3) *Pressure pulse*: The high pressure building up in the high-energy-density region drives the material radially out. Particles which acquire enough momentum to surpass the surface barrier are emitted.[17]

(4) *Shock waves*: The shock wave emitted from the track volume may eject matter when unloading at the surface.[19,20]

It was shown in Ref. 16 that the various models for the ejection process are related to each other, each expressing an aspect of the continuum mechanical behavior of materials at high-energy density. Here we note again that the yield can quite generally be written as

$$Y \cong n_0(\pi\overline{R^2})\overline{\Delta z} \ , \tag{8}$$

where $\pi\overline{R^2}$ is a mean area and $\overline{\Delta z}$ a mean depth, with their various dependencies given in Ref. 16.

In the present simulations, we find at high-energy densities ($E_0 \gtrsim U$) that $\pi\overline{R^2} \propto \pi R_0^2$, as suggested in the gas-flow calculation of Ref. 14, whereas $\overline{\Delta z} \propto E_0/U$, cf. Eq. (2). At low $dE/dx$ ($E_0/U$ small or $R_0/l$ large), $\pi\overline{R^2} < \pi R_0^2$ with $\pi\overline{R^2} \propto (E_0/U)^2$.

The result for $\overline{\Delta z}$ can be understood via the thermal-spike or gas-flow model. There, it is $\overline{\Delta z} \propto \Delta t$, the time for sustaining $E_0/U > 1$. Even though radial conductivity is low, the cylinder will evacuate material until the transport of energy/momentum either radially or to the "substrate" below the track terminates the flow. Therefore $\Delta t \propto (E_0/U)\cdot(L_T/v_T)$, where $L_T$ is a transport length and $v_T$ is a transport speed. For radial energy transport, since the area is $4\pi R_0^2$ and the boundary $2\pi R_0$, $L_T/v_T \cong (R_0/2)\cdot(l/k)$, where $\kappa$ is the diffusivity at ambient temperature. The slower than linear dependence of $\overline{\Delta z}$ on $R_0$ suggests that both substrate and radial energy/momentum transport probably participate in determining $\Delta t$.

The standard (and misnamed) "thermal-spike" model is similar to gas flow; in the latter, however, the average molecule energy is usually allowed to significantly exceed $U$, in which case the standard vapor pressure relationship breaks down, as has been pointed out and accounted for often. However, in all such models (for $R_0/l$ small) in the cylindrical geometry the only loss of energy is radial. That is, the energy/momentum carried off by the molecules is *not* accounted for (see, however, Ref. 41). By fixing $\pi\overline{R^2}$, as in Ref. 14, the authors essentially account for this, although their calculation leads to $\overline{\Delta z} \propto \sqrt{E_0/U - 1}$. It is also seen that the concern expressed in Ref. 16 that if $\overline{\Delta z}$ became significantly larger than $\overline{R}$, as it can in the spike and gas-flow models, the pressure in the cylinder would "blow off" the edges of the crater creating a more hemispherical volume, does not occur here. That is, quite large depths can be evacuated with relatively small radii. This happens since at larger depths, particles leave the excitation track primarily in radial direction, i.e., into the surrounding material. The relaxation of this compressed region could lead to further ejection at long times, but that is not expected to change the picture much.

Within the "shock" and "pressure-pulse" models the one-dimensional ejection could also be understandable. That is, at small $dE/dx$ the radial scale for effectively transferring momentum to the surface atoms grows with increasing $dE/dx$. However, after transmitting the initial shock, the radial pressure acts only to slightly enlarge the cylinder, whereas the pressure gradient along the $z$ direction effectively couples into motion in the $z$ direction, producing material expansion. In fact, the evidence in Fig. 4(c) is that at high $dE/dx$, radial compression is the limiting effect. This effectively one-dimensional expansion should have strong parallels with the effectively one-dimensional, probably isentropic, expansion produced by laser excitation of the surface, for which $\pi R_0^2$ is the pulse area and $\overline{\Delta z}$ is determined by the absorbance profile.[43]

We note that the changing dependence of the volume of the ejecta on the energy deposited also occurs for micrometeorite impact of surfaces. A steep slope is seen at low-energy densities deposited, but the ejecta volume becomes nearly proportional to the energy deposited at high-energy densities. The latter dependence is that expected from scaling arguments.[44]

In conclusion, the following picture emerges. At the lowest excitation densities, particles are emitted from the first monolayer and originate from the track itself. The scaling of the yield in this regime can probably be best understood within the pressure pulse model, where it is argued that the radial and depth dimensions of the ejection volume scale like $dE/dx$, i.e., like $E_0/U$.[45] Above the critical energy density of $E_0/U$, particles still come predominantly from the track region. This shows that the phase of the material is of importance; the cold, solid environment of the track strongly resists particle ejection,

and it does not undergo a phase transformation in the system studied by us. This issue is well taken into account by the gas-flow model. The depth scale from which particles are ejected is then determined by heat conduction and thinning of the track volume by radial expansion. Pressure pulse concepts may as well apply here. If emission is restricted to the track region itself, only the depth scale depends on the energy density, and it scales linearly with $E_0/U$.

## IV. CONCLUSIONS

We presented molecular-dynamics results on particle emission from a cylindrically excited track in a condensed rare-gas target. The low number of parameters (viz. the binding energy and length) allowed a systematic study of the ejection yield.

An idealized model is used. All atoms in the track are given a fixed energy $E_0$, but random direction of motion. The existence of charged species (electrons and ions) in the track as well as a smooth radial gradient in the energy deposition is disregarded as is the case in earlier calculations by others. In addition, calculations are terminated around 20 ps, although in some cases considerable relaxation may occur at larger times, possibly accompanied by sublimation.

The time evolution of the target material in and around the cylindrical track shows a simple and characteristic behavior which is largely independent of the track size and energy. The large pressure built up inside the track leads to the propagation of a shock wave which travels radially into the cold target material. As a consequence, the shocked material propagates radially outward, and the target density in the track and its surroundings sinks. The huge temperature in the track quickly sinks due to heat conduction and expansion, and—close to the surface—due to ejection cooling. Even for quite energetic tracks (track particle energy equal to twice the cohesive energy), the material surrounding the track is not heated sufficiently to become fluid; i.e., for the most part its temperature remains below the critical point of the liquid-gas phase transition. For high-energy-density tracks, the expansion of the track is so strong that it is depleted of matter and a deep, but transient, crater has formed at the end of the simulation.

Material is ejected from the track into the vacuum above the surface due to the large transient pressure gradient in the outwards direction. Particles are ejected from the first few monolayers only, even at high energy densities. The yield is found to be proportional to the cross section area of the cylinder at the surface at high energy densities. Two regimes are identified: If the energy per track particle $E_0$ is below the cohesive energy $U$ of the material, the yield rises roughly like the third power of $E_0$ (cubic or threshold regime); for $E_0 \gtrsim U$, it rises only linearly (linear regime).

An analysis of the emitted particles shows that these indeed predominantly originate from the track itself. The angular distribution is strongly peaked in the direction of the outward surface normal, demonstrating that the huge pressure in the track is the driving force for directed motion. The energy distribution of particles ejected from a high-energy-density track shows a considerable number of particles ejected with kinetic energies in excess of their initial track energies. Therefore interparticle collisions are active in the ejection process, either in the condensed phase during ejection or in a briefly collisional jet.

The following picture emerged. In the low-energy-density regime, particles are emitted from the first monolayer and originate from the track itself. Above the critical energy density of $E_0/U$, particles still come predominantly from the track region only, and from the first few monolayers. This suggests that the phase of the material is of importance; the cold, solid environment of the track strongly resists particle ejection, and it does not undergo a phase transformation in the system studied by us. The depth scale from which particles are ejected is then determined by radial compression and by the decay of the pressure towards greater depths.

## ACKNOWLEDGMENTS

We gratefully acknowledge the help of K. T. Waldeer, who wrote the molecular-dynamics code and was instrumental in initiating this work. R.E.J. acknowledges the support of the National Science Foundation.

[1]R. L. Fleischer, P. B. Price, and R. M. Walker, *Nuclear Tracks in Solids* (University of California, Berkeley, 1975).

[2]B. U. R. Sundqvist, in *Sputtering by Particle Bombardment III,* edited by R. Behrisch and K. Wittmaack (Springer, Berlin, 1991), Chap. 5, p. 257.

[3]*Desorption Induced by Electronic Transitions DIET I,* edited by N. H. Tolk, M. M. Traum, J. C. Tully, and T. E. Madey, Springer Series in Chemical Physics, Vol. 24 (Springer, Heidelberg, 1983).

[4]*Desorption Induced by Electronic Transitions DIET II,* edited by W. Brenig and D. Menzel, Springer Series in Surface Sciences, Vol. 4 (Springer, Heidelberg, 1985).

[5]*Desorption Induced by Electronic Transitions DIET III,* edited by R. H. Stulen and M. L. Knotek, Springer Series in Surface Sciences, Vol. 13 (Springer, Heidelberg, 1988).

[6]*Desorption Induced by Electronic Transitions DIET IV,* edited by G. Betz and P. Varga, Springer Series in Surface Sciences, Vol. 19 (Springer, Berlin, 1990).

[7]R. E. Johnson, *Energetic Charged-Particle Interactions with Atmospheres and Surfaces* (Springer, Berlin, 1990).

[8]B. E. Fischer and R. Spohr, Rev. Mod. Phys. **55**, 907 (1983).

[9]D. F. Torgerson, R. P. Skowronski, and R. D. Macfarlane, Biochem. Biophys. Res. Commun. **60**, 616 (1974).

[10]R. E. Johnson, in *Proceedings of Ion Formation from Organic Solids V (IFOSV),* edited by A. Hedin, B. U. R. Sundqvist, and A. Benninghoven (Wiley, Chichester, 1990), p. 189.

[11]R. E. Johnson, S. Banerjee, A. Hedin, D. Fenyö, and B. U. R. Sundqvist, in *Ion Formation from Organic Solids,* edited by W. Ens and K. Standing (Plenum, New York, 1991), p. 89.
[12]R. E. Johnson and B. U. R. Sundqvist, Phys. Today **45**(5), 28 (1992).
[13]P. Sigmund and C. Claussen, J. Appl. Phys. **52**, 990 (1981).
[14]H. M. Urbassek and J. Michl, Nucl. Instrum. Methods B **22**, 480 (1987).
[15]W. L. Brown and R. E. Johnson, Nucl. Instrum. Methods B **13**, 295 (1986).
[16]R. E. Johnson, Int. J. Mass Spectrom. Ion Phys. **78**, 357 (1987).
[17]R. E. Johnson, B. U. R. Sundqvist, A. Hedin, and D. Fenyö, Phys. Rev. B **40**, 49 (1989).
[18]D. Fenyö, B. U. R. Sundqvist, B. R. Karlsson, and R. E. Johnson, Phys. Rev. B **42**, 1895 (1990).
[19]I. S. Bitensky and E. S. Parilis, Nucl. Instrum. Methods B **21**, 26 (1987).
[20]I. S. Bitensky, A. M. Goldenberg, and E. S. Parilis, J. Phys. (Paris) Colloq. **50**, C2-213 (1989).
[21]J. Michl, Int. J. Mass Spectrom. Ion Phys. **53**, 255 (1983).
[22]S. Banerjee, R. E. Johnson, S. Cui, and P. T. Cummings, Phys. Rev. B **43**, 12 707 (1991).
[23]Y. Wu and R. J. Friauf, J. Appl. Phys. **65**, 4714 (1989).
[24]C. Kittel, *Introduction to Solid State Physics* (Wiley, New York, 1971).
[25]K. T. Waldeer and H. M. Urbassek, Nucl. Instrum. Methods B **73**, 14 (1993).
[26]G. S. Grest, B. Dünweg, and K. Kremer, Comput. Phys. Commun. **55**, 269 (1989).
[27]Y. Fujii, N. A. Lurie, R. Pynn, and G. Shirane, Phys. Rev. B **10**, 3647 (1974).
[28]J. Grindlay and R. Howards, in *Lattice Dynamics,* edited by R. F. Wallis (Pergamon, Oxford, 1965), p. 129.
[29]P. Brüesch, *Phonons: Theory and Experiments I,* Springer Series in Solid State Sciences, Vol. 34 (Springer, Berlin, 1982).
[30]N. W. Ashcroft and N. D. Mermin, *Solid State Physics* (Saunders, Philadelphia, 1976).
[31]L. Verlet, Phys. Rev. **159**, 98 (1967).
[32]C. Y. Ho, R. W. Powell, and P. E. Liley, J. Phys. Chem. Ref. Data **1**, 279 (1972).
[33]J.-P. Hansen and L. Verlet, Phys. Rev. **184**, 151 (1969).
[34]Y. B. Zel'dovich and Y. P. Raizer, *Physics of Shock Waves and High-Temperature Hydrodynamic Phenomena* (Academic, New York, 1967), Vol. 2.
[35]H. M. Urbassek and K. T. Waldeer, Phys. Rev. Lett. **67**, 105 (1991).
[36]D. Fenyö and R. E. Johnson, Phys. Rev. B **46**, 5090 (1992).
[37]P. Sigmund, Appl. Phys. Lett. **25**, 169 (1974); **27**, 52 (1975).
[38]R. E. Johnson and R. Evatt, Radiat. Eff. **52**, 187 (1980).
[39]O. Ellegaard, J. Schou, and H. Sørensen, Europhys. Lett. **12**, 459 (1990).
[40]O. Ellegaard, J. Schou, B. Stenum, H. Sørensen, and R. Pedrys, Nucl. Instrum. Methods **B62**, 447 (1992).
[41]M. Urbassek and P. Sigmund, Appl. Phys. A **35**, 19 (1984).
[42]V. Balaji, D. E. David, T. F. Magnera, J. Michl, and H. M. Urbassek, Nucl. Instrum. Methods B **46**, 435 (1990).
[43]R. E. Johnson and B. U. R. Sundqvist, Rapid Commun. Mass Spectrom. **5**, 574 (1991).
[44]A. J. Chabai, J. Geophys. Res. **70**, 5075 (1965).
[45]The model as derived (Refs. 17 and 36) is for a narrow track. Recently this was extended to tracks with significant width exhibiting a shallower ejection volume [D. Fenyö, Phys. Rev. B **47**, 8263 (1993)].
[46]Mean interparticle distance $l = 24$ Å [D. Fenyö (private communication)].